OPTICAL SURFACE CONTOURING FOR NON-DESTRUCTIVE INSPECTION OF TURBOMACHINERY

R&D STATUS REPORT #1

For the period
6 December, 1993 - 5 February, 1994

Contract No.
NAS3-27214
PR I # 200

9 March, 1994

Prepared by:

Dariush Modarress and David F. Schaack
Physical Research, Inc.
25500 Hawthorne Boulevard, Suite 2300
Torrance, California 90505-6828

Prepared for:

NASA Lewis Research Center
Attention: Ms. Carolyn Mercer, Technical Monitor
Cleveland, Ohio 44135

1.0 INTRODUCTION

Detection of stress cracks and other surface defects during maintenance and in-service inspection of propulsion system components, including turbine blades and combustion compartments, is presently performed visually. There is a need for a non-contact, miniaturized, and fully fieldable instrument that may be used as an automated inspection tool for inspection of aircraft engines.

During this SBIR Phase I program, the feasibility of a ruggedized optical probe for automatic and non-destructive inspection of complex shaped objects will be established. Through a careful analysis of the measurement requirements, geometrical and optical constraints, and consideration of issues such as manufacturability, compactness, simplicity, and cost, one or more conceptual optical designs will be developed. The proposed concept will be further developed and a prototype will be fabricated during Phase II.

2.0 SUMMARY OF RESEARCH EFFORT

This progress report summarizes work performed since the start of the contract on the feasibility of one or more optical surface inspection techniques and is reported according to each task performed.

Task 1. Identification of Instrument Specification

During the reporting period, a number of commercial, Government, and military engine repair and maintenance organizations were visited. Based on these visits and other sources of information, a preliminary report on the identification of one or more suitable optical surface inspection instrument has been prepared and is included in the Appendix 1.

Task 2. Conceptual Design of the Probe Optical System

The purpose of this task was to generate the mathematical analysis of the interference fringe projection contouring process for an arbitrary geometry, and use the model to help develop a conceptual model of an optical non destructive instrumentation.

Work on this task has been initiated by Dr. Schaack. Preliminary reports dated 2/11/94 and 3/3/94 have been generated and are included in the Appendix 2.

Task 3. Identify Candidate Hardware Elements for the Instrument

No work was performed under this task.

Task 4. Evaluation of Instrument Feasibility

No work was performed under this task.

Summary

Percentage of tasks completed and the expected date of completion are shown herein:

TASKS	PERCENTAGE ACCOMPLISHED	EXPECTED COMPLETION DATE
TASK 1	80%	4/30/94
TASK 2	30%	4/30/94
TASK 3	0%	5/15/94
TASK 4	0%	6/5/94
TASK 5	15%	6/5/94

Percentage of physical completion of the contract was estimated at 24.0%.

Total cumulative costs incurred as of the report date was $18,800 , or 28.5% of the total contract funds.

Cumulative cost to complete the contract is estimated at $65,771, or 100% of the total contract funds.

3.0 FUTURE WORK

Work planned for the next reporting period is to complete Task 1, Task 2 and Task 3.

APPENDIX 1

Preliminary Report on Task 1.

Purpose: The purpose of this task was to determine the specifications and the requirements for one or more optical techniques for non-destructive inspection of surfaces with arbitrary shapes.

Market Segment:

The scope of the survey was limited to the aircraft engine inspection and maintenance organizations. This market segment was best known to us as a result of our marketing of the MOI. Furthermore, a successful development of an optical non-destructive instrument for this market could be immediately introduced in the market using our existing sales and marketing network.

During the reporting period we visited a number of commercial, Government, and military engine repair and maintenance organizations. Additional telephone interviews were carried out with the aircraft engine manufacturers.

Market Requirements:

Preliminary results of our survey pointed to two different inspection needs in the commercial and the military markets. The most immediate need in the commercial and military aircraft engine inspection market is for an instrument to provide the dimensions of defects that are visually located through a borescope. This instrument may be used in conjunction with borescopes primarily for in-service inspection of aircraft engines.

The second inspection requirements identified was for automated detection of surface cracks. This instrument has an immediate application in the aircraft engine overhaul market.

In-Service Aircraft Engine Inspection:

These inspections are carried out every 200 to 300 hours of operation. Borescopes are used to visually determine the integrity of the engines' internal components such as compressor and turbine blades, engine linings, and combustor areas. Inspectors look for two types of damage: 1) missing components and 2) foreign object impact damage. When a defect is detected, it is necessary to estimate the defect's size. The engines are removed from the wing when damage beyond a pre-specified size is detected. Unscheduled and unnecessary engine removal and tear down is expensive in both labor and downtime for the aircraft. More accurate determination of the defect size over curved surfaces (e.g. turbine or compressor blades) result in large cost savings.

The majority of borescopes commonly used do not have the capability to perform in-situ measurement. Direct measurement generally involves tools or scales of known dimension fed through a separate port hole in the engine, or through a working channel in the scope, and placed in the work site for comparison with the defect. The method relies heavily on subjective interpretation of the measurement. There is no correction for curved surfaces. When a borderline defect is detected, one or more inspectors with extensive experience are summoned to make the final determination.

Market Size:
A preliminary review of the size of the potential market for an optical instrument successfully developed for aircraft in-service inspection was conducted. The list of companies and organizations categorized as possible end users was extracted from the available directories. Categories that were included in the data base included airplane and helicopter manufacturers, U.S. airlines, non-U.S. airlines, non-airline engine service and maintenance organizations, spacecraft and launch vehicle manufacturers, U.S. military, and foreign military. The total aircraft market size for the proposed optical instrument was estimated to be between 2,000 to 5,000 units. The size of other non-aircraft markets was estimated at about 1,000 units. For a sales price of $15,000 per instrument (an upper limit, based on our interviews), the total market was valued at $45M to $90M.

Competitions:
Presently there are only two instruments that are commercially available and address this requirement: the Olympus IW-1 Video Analyzer, and the Welch Allyn ShadowProbe.

The Video Analyzer is a combination of an image manipulator program with a large data base containing the surface profiles of a number of compressor and turbine blades. The input to the program is a borescope image of a blade (with a defect) digitized by an image grabber, and the part number of the blade entered by the operator. The program then generates a mesh of known dimensions and overlays the blade image. This instrument costs $25,000, and over 200 units have been sold in the U.S. The air lines and the maintenance organizations visited did not purchase this unit primarily due to its cost and its limitations in its applications.

The ShadowProbe is a specialized borescope that optically projects a calibrated scale of known dimensions onto the inspection surface. It measures the distance along the surface. It can also measure the depth variation associated with a crack or other surface defects. Its accuracy, however, is poor for highly curved surfaces. The instrument cost is $40,000. The locations visited were all aware of this instrument, but chose not to acquire the product. Reasons included the price, and the fact that it was not compatible with their existing line of borescopes.

User Requirements:
The requirements identified based on the survey are listed herein:

a) The instrument should either operate as a borescope, or be designed as an attachment to existing borescopes. Side projected 8 or 10 mm rigid borescopes are used in the majority of the in-service inspections and should be considered as an initial design target.
b) Object distance from the side of the borescope: a few millimeter to 10 cm. (Depth of field of borescopes are from 0 to ∞)
c) Field of view: 55° to 60°.
d) Minimum defect size: 0.3 mm (0.01)"
b) The measurement accuracy of defect size: +/- 0.1 mm (0.005")
c) Depth accuracy: +/- 0.1 mm (0.005") for sizes up to 3 mm (0.1").
d) Ruggedized design
e) Priced for under $15,000.

Automated Crack Detection:

Military and commercial aircraft engine tear down is routinely performed according to a pre-defined schedule. Partial engine repair is also performed when a defective part is detected. There is an immediate need for an automated crack detector for the compressor and turbine blades of military engines. Liquid penetrant is presently used. Each item is manually inspected in dark rooms. The commercial engines do not have the same requirements.

Market Size: TBD

Competitions:

There is presently no commercial product that may be used to automatically detect small surface cracks with high degree of certainty and reliability.

User Requirements:

Automated crack detection may be used in conjunction with a liquid penetrant technique. Here, the samples are cleaned, immersed in liquid penetrant, cleaned and looked at under UV light. Automated tools exist to identify areas with high UV light scatter. Automated crack detection is required to identify cracks vs. others such as surface scratches, lint, tar, etc.

Other requirements are summarized as follows:

a) Material: metal
b) Coating: varied
c) Inspection area size: 5 mm x 5 mm (0.2" x 0.2")
c) Overall sample size: 25 cm x 25 cm (10" x 10")
d) Crack length: 0.1 mm (0.03")
e) Shape: varied

Appendix 2

Preliminary Report on Task 2.

MEMO: 2/11/94
TO: Dariush Modarress, Physical Research
FROM: David F. Schaack, Consulting Engineer
SUBJECT: Local Height Sensitivity in Projected Fringe Surface Contouring I. A Preliminary Analysis

Scope

Since we wish to investigate the use of the projected fringe surface contouring for in-situ inspection of turbine blades, we must consider the constraints imposed by the unusual inspection geometry. To enable us to do this, we need a general model of the projected fringe contouring process. As one of the first steps toward development of this model, I here derive an expression for the relationship between the height change of a surface and the shift of the fringe intersection with the surface as viewed along an arbitrary direction. This expression is more general than any I have seen previously, and I use it to derive a previously reported result. I also briefly explain the limitations of this expression as a preliminary to the next report of this series.

Introduction

The general problem of analyzing the geometry of projected fringe contouring involves the use of a pair of coherent light sources to form a set of hyperboloidal fringes in space. Into this fringe field is introduced an arbitrary surface of interest at some position of interest. The resulting illumination of the surface is viewed from some other position of interest, and the illumination pattern on the camera focal plane is calculated.

In general, the most complicated element of the general model just described is the surface under observation. The reasons that we consider it such are that it may have an arbitrary surface contour which is complicated to describe, and that the key direction which is to be considered "surface height", is determined solely by the definition of the surface. Thus, it makes sense to base the general analysis model on a coordinate system which is defined relative to the surface under test. This means that the fringe sources and fringe observation system should be considered to be located at any arbitrary position with respect to the surface.

In the development of the general model it is important and helpful to have an understanding of the characteristics of the system in particular limiting cases. Such understanding can guide one toward attractive design alternatives which can then be analyzed in detail by use of the general model.

In this document, I analyze the operation of a projected fringe contouring system in the limit in which the entrance pupil of the camera is at a large distance from the surface. This means that we need not consider the effect of perspective distortion on the imaging of the surface illumination pattern. We also assume that the sources are at a large distance from the surface under test. This assumption means that the fringe field is considered to be a series of parallel planes. We further restrict the analysis to a small portion of the surface which can be considered to be a plane. Note that the latter two restrictions are not very severe; any portion of any surface in any fringe field could be analyzed in this way, it is just that an arbitrary surface in an arbitrary field would have to be analyzed in a piecewise fashion.

Analysis

Figure 1 shows two point sources forming a field of planar fringes at a large distance R_s. If the spacing between the sources is 2d, the spacing between the fringes is:

$$\delta_f = \frac{\lambda R_s}{2d} \tag{1}$$

In figure 2 is shown the fringe field with a unit vector $\hat{s}$ perpendicular to the fringe planes. This vector completely specifies the orientation of the fringes. Also shown is a plane surface with its unit normal $\hat{n}$, at some arbitrary orientation.

In figure 3 is shown the intersection of the fringe planes with the surface as viewed perpendicular to the plane containing both $\hat{s}$ and $\hat{n}$. We define δ_p as the spacing of the fringe intersections with the surface as measured in the plane of the surface. Since the fringe planes make an angle θ with the surface:

$$\sin(\theta) = \frac{\delta_f}{\delta_p} \tag{2}$$

or

$$\delta_p = \frac{\delta_f}{\sin(\theta)} = \frac{\delta_f}{|\hat{n} \times \hat{s}|} \tag{3}$$

The loci of the fringe intersections with the surface are lines which are perpendicular to the plane of figure 3, that is, these lines are parallel to the vector $\hat{n} \times \hat{s}$. Figure 4 shows a view of the surface in which the unit vector $\hat{a}$ is oriented parallel to the lines of fringe intersection:

$$\hat{a} = \frac{\hat{s} \times \hat{n}}{|\hat{s} \times \hat{n}|} \tag{3a}$$

The direction that also lies in the plane of the surface but that is perpendicular to the fringe intersections is parallel to $\hat{b}$:

$$\hat{b} = \frac{\hat{n} \times (\hat{s} \times \hat{n})}{|\hat{s} \times \hat{n}|} = \frac{\hat{s} - (\hat{n} \cdot \hat{s})\,\hat{n}}{|\hat{s} \times \hat{n}|} \tag{4}$$

Thus $\hat{b}$ lies in the plane containing $\hat{s}$ and $\hat{n}$, and it is also shown in Figure 4.

Here we define the direction for surface height changes as being along $\hat{n}$. Figure 5 shows what occurs if the surface moves a distance ε in the height direction. The figure is drawn in the plane containing $\hat{s}$ and $\hat{n}$. What happens is that the intersection of a particular physical fringe with the surface moves from point A to point B. If we define a unit vector $\hat{\eta}$ in this direction, it clearly will have no component perpendicular to the figure, which is the $\hat{s} \times \hat{n}$ direction. It also clearly has no component parallel to $\hat{s}$. Thus:

$$\hat{\eta} = \hat{a} \times \hat{s} = \frac{\hat{s} \times (\hat{n} \times \hat{s})}{|\hat{s} \times \hat{n}|} = \frac{\hat{n} - (\hat{n} \cdot \hat{s})\,\hat{s}}{|\hat{s} \times \hat{n}|} \tag{5}$$

Note that this vector lies in the plane of the fringes.

The magnitude of the movement of the fringe intersection is:

$$p = \frac{\varepsilon}{\sin\theta} = \frac{\varepsilon}{|\hat{s} \times \hat{n}|} \tag{6}$$

so that the physical motion of the fringe intersection can be represented as a vector:

$$\vec{f} = p\,\hat{\eta} = \frac{\varepsilon\,\hat{\eta}}{|\hat{s} \times \hat{n}|} \tag{7}$$

Now consider that the surface is being viewed along an arbitrary direction defined by the unit vector $\hat{c}$ (not shown). As a consequence, the fringe motion $\vec{f}$ is also viewed

along that direction. The resulting fringe image motion as projected on the viewing plane will be equal to the component of $\vec{f}$ which lies in the plane perpendicular to the viewing direction, $\hat{c}$ (we assume a viewing magnification of 1).

The component of $\vec{f}$ which is perpendicular to $\hat{c}$ is simply given by the difference between $\vec{f}$ and the component of $\vec{f}$ which is **parallel** to $\hat{c}$. That is:

$$\vec{v} = \vec{f} - (\vec{f} \cdot \hat{c})\,\hat{c} = p\left[\hat{\eta} - (\hat{\eta} \cdot \hat{c})\,\hat{c}\right] \tag{8}$$

is the vector which gives the fringe motion as projected onto the viewing plane. Plugging in the expressions for $\vec{f}$ and $\hat{\eta}$ we find:

$$\vec{v} = \varepsilon\left\{\frac{\left[\hat{n} - (\hat{n}\cdot\hat{s})\,\hat{s} - \left[(\hat{n} \cdot \hat{c}) - (\hat{n} \cdot \hat{s})(\hat{s} \cdot \hat{c})\right]\hat{c}\right]}{|\hat{s} \times \hat{n}|^2}\right\} \tag{9}$$

Equation (9) is the main result of this memo. It gives the apparent motion of a fringe intersection with the surface as viewed along an arbitrary direction $\hat{c}$, when the surface is translated a distance ε along its normal $\hat{n}$, and the surface is illuminated with a set of plane-parallel fringes perpendicular to $\hat{s}$.

Application

From (8) it is clear that $\vec{v}$ will be zero if $\hat{c} = \pm\hat{\eta}$; that is, the fringe motion is not visible if the view is along the plane of the fringes and lies in the plane containing $\hat{n}$ and $\hat{s}$. If one resolves (8) into components along the x, y, and z directions it is easy to show that:

$$|\vec{v}|^2 = p^2\left[1 - (\hat{\eta} \cdot \hat{c})^2\right] \tag{10}$$

i.e., that the apparent motion of the fringe as viewed is maximized when the view is perpendicular to $\hat{\eta}$.

View Perpendicular to Surface

If the view is constrained to be perpendicular to the surface, $\hat{c} = -\hat{n}$ and (9) becomes:

$$\vec{v} = \varepsilon \left\{ \frac{\left[\hat{n} - (\hat{n} \cdot \hat{s})\, \hat{s} - \hat{n} + (\hat{n} \cdot \hat{s})^2\, \hat{n} \right]}{|\hat{s} \times \hat{n}|^2} \right\} \tag{11}$$

or

$$\vec{v} = \varepsilon \left\{ \frac{\hat{n} \cos\theta - \hat{s}}{\sin\theta \tan\theta} \right\} \tag{12}$$

where θ has been defined in figures 3 and 5. Considering the magnitude of $\vec{v}$, we find:

$$|\vec{v}| = \frac{\varepsilon}{\tan\theta} \tag{13}$$

This tells us that the maximum sensitivity is obtained by making the surface nearly parallel to the fringes, when the view is perpendicular to the surface.

It may well be that a certain instrument has a resolution best described in terms of a minimum resolvable phase shift, $\Delta\phi$. Since the view is perpendicular to the surface, the spacing of the fringes as viewed will be the same as the physical spacing on the surface, which was defined previously as δ_p. In this case, we can write the phase shift in terms of the apparent fringe motion as:

$$\Delta\phi = 2\pi \frac{|\vec{v}|}{\delta_p} = 2\pi \frac{\varepsilon}{\tan\theta\, \delta_p} \tag{14}$$

The surface height change in terms of the phase shift is:

$$\varepsilon = \frac{\delta_p}{2\pi} \tan\theta\, \Delta\phi \tag{15}$$

which matches Equation (2) of NASA Technical Memorandum 103252, by Mercer and Beheim.

It is important to note that while (14) and (15) promise a high gain in sensitivity by orienting the surface nearly parallel to the fringe pattern, that gain in sensitivity may not be attainable because of a hidden assumption. In those equations, the physical spacing of the fringe intersections along the surface, δ_p, is considered constant as the

angle of the surface is varied. In order for this to happen, the physical spacing of the fringe pattern, δ_f, must be varied with angle; in fact, (2) shows that it must be proportional to $\sin\theta$. If for some reason the fringe spacing is restricted to some minimum value then the appropriate expression for height sensitivity is:

$$\frac{\Delta\phi}{\varepsilon} = \frac{2\pi}{\delta_f^{min}} \cos\theta \tag{16}$$

and the increase in sensitivity as θ is made small is much less impressive. In fact, expression (16) is the one appropriate for our purpose, since we will be trying to contour objects lying at various orientations with an instrument that will have little or no ability to vary δ_f.

Limitations

The problem with expression (9) is that it gives the physical shift of the fringe intersection, not the phase shift. Since we will be measuring the phase shift, we need a general expression for that, based on (9). It turns out that deriving, checking and applying the resulting expression is a long story -- long enough to merit its own document. This will be the subject of the next report in this series.

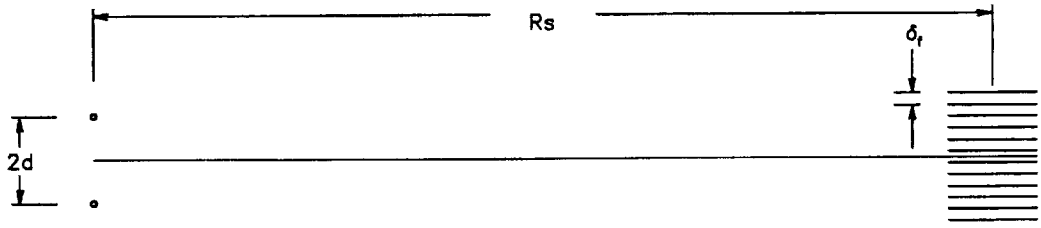

Fringe planes formed by a pair of sources.

FIGURE 1

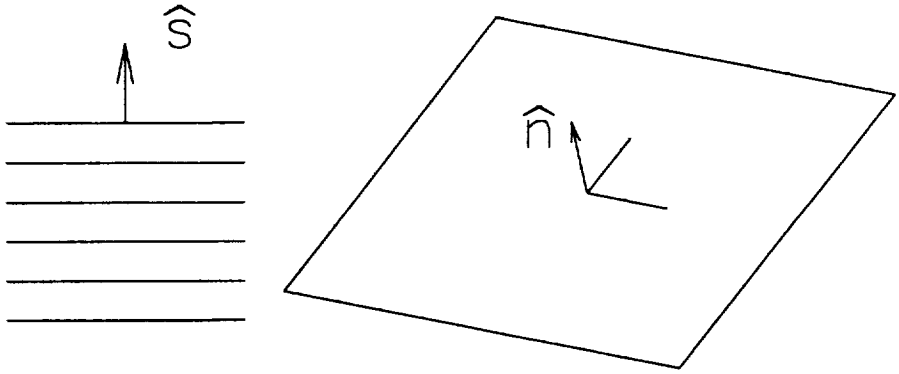

Fringe surfaces intersecting with a plane.

FIGURE 2

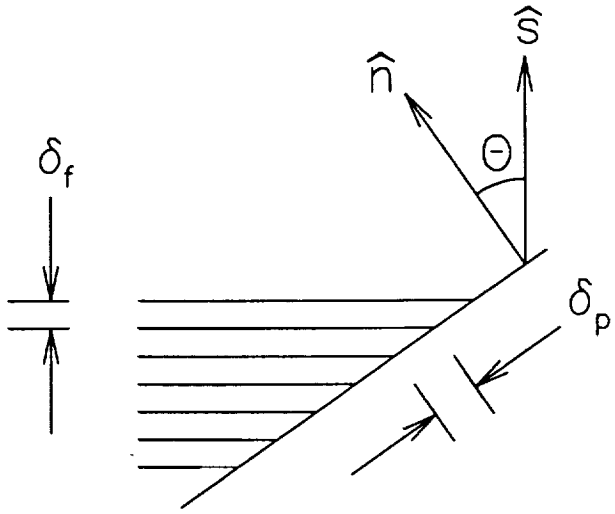

Intersections of fringes with surface.

FIGURE 3

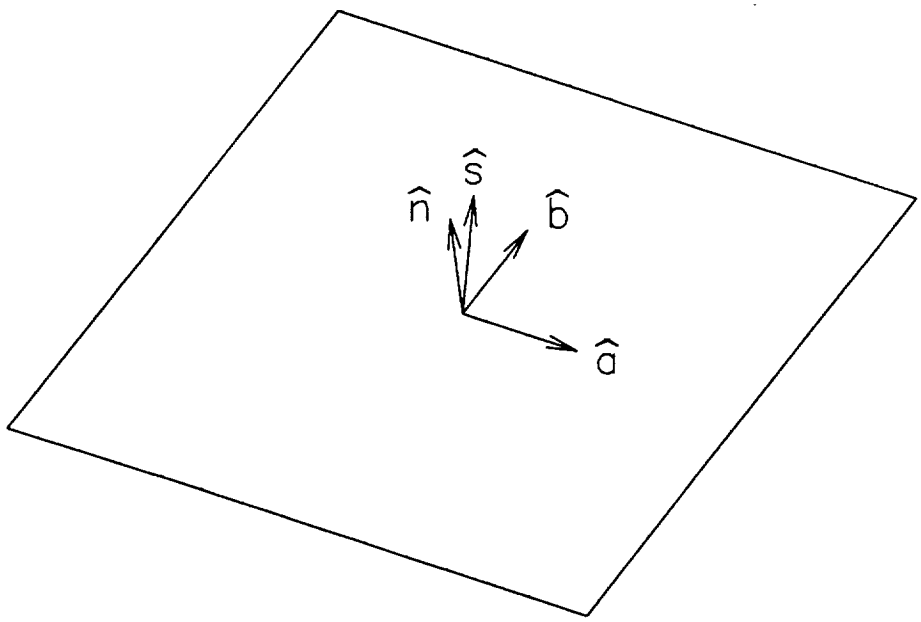

Unit vectors defined at the surface.

FIGURE 4

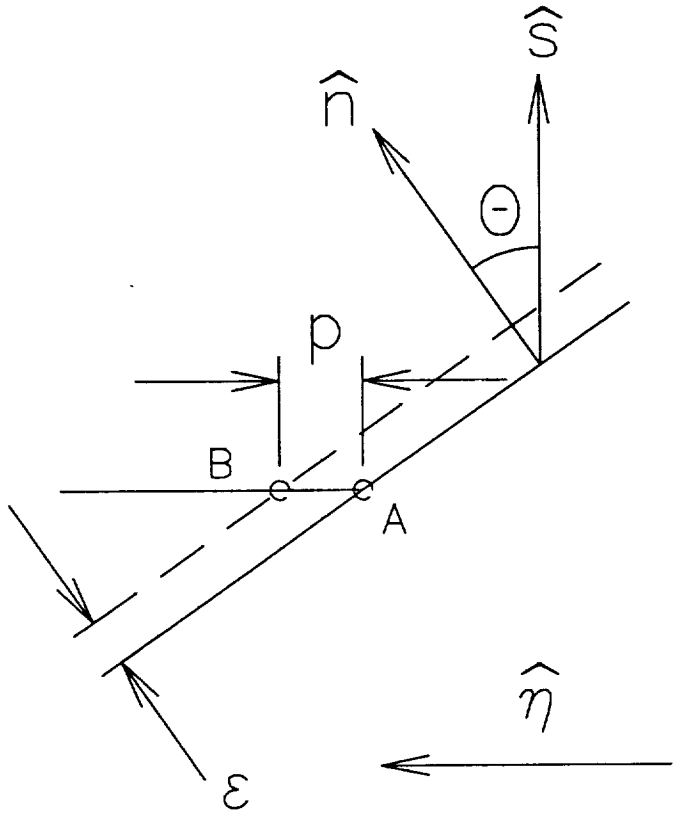

Change in fringe intersection at surface.

FIGURE 5

MEMO: 3/3/94
TO: Dariush Modarress, PRi
FROM: David F. Schaack, Consulting Engineer
SUBJECT: Local Height Sensitivity in Projected Fringe Surface Contouring II. Determination of the Phase Shift

Introduction

In the first report of this series, dated 2/11/94 and referred to here as "Sensitivity I." , I derived an expression for the shift of the fringe intersection with the surface as viewed from an arbitrary direction. In this report, I derive a general expression for the phase shift.

As a reminder, these reports analyze the operation of a projected fringe contouring system at the limit in which the entrance pupil of the camera is at a large distance from the surface. Thus, we are not considering the effect of perspective distortion on the imaging of the surface illumination pattern. We also are assuming that the sources are at a large distance from the surface under test. This means that the fringe field is considered to be a series of parallel planes. We have also restricted the analysis to a small portion of the surface which can be considered to be a plane. As stated previously, the latter two restrictions are not very severe; any portion of any surface in any fringe field could be analyzed in this way, it is just that an arbitrary surface in an arbitrary field would have to be analyzed in a piecewise fashion.

Analysis

Figure 1 shows a view of a planar surface with a field of fringe planes intersecting it. The fringe planes have been partially cut away so that the lines of intersection between the fringe planes and the surface are visible. Also visible is the set of unit vectors which specify the geometry. These vectors were defined in Sensitivity I. ; here I summarize their definitions.

The vector $\hat{n}$ is the unit normal of the surface being inspected. The orientation of the parallel set of fringe planes is denoted by the unit normal $\hat{s}$. The lines of intersection of the fringes with the surface are parallel to the vector $\hat{a}$ and perpendicular to $\hat{b}$. These vectors lie in the surface and are derived from $\hat{n}$ and $\hat{s}$ by:

$$\hat{a} = \frac{\hat{s} \times \hat{n}}{|\hat{s} \times \hat{n}|} \tag{1}$$

and

$$\hat{b} = \frac{\hat{n} \times (\hat{s} \times \hat{n})}{|\hat{s} \times \hat{n}|} = \frac{\hat{s} - (\hat{n} \cdot \hat{s})\,\hat{n}}{|\hat{s} \times \hat{n}|} \tag{2}$$

The vector $\hat{\eta}$ lies in the plane of the fringes and also in the plane containing $\hat{n}$ and $\hat{s}$. It denotes the direction which the fringe intersection moves if the surface changes height.

$$\hat{\eta} = \hat{a} \times \hat{s} = \frac{\hat{s} \times (\hat{n} \times \hat{s})}{|\hat{s} \times \hat{n}|} = \frac{\hat{n} - (\hat{n} \cdot \hat{s})\,\hat{s}}{|\hat{s} \times \hat{n}|} \tag{3}$$

It is important to realize that the apparent geometrical relationships between these vectors varies as these vectors are viewed from different directions. In particular, notice that in Figure 1, $\hat{a}$ and $\hat{b}$ do not appear to be mutually perpendicular nor do $\hat{s}$, $\hat{n}$ or $\hat{\eta}$ appear to be perpendicular to $\hat{a}$. It is the apparent relationships between these vectors as seen in the viewing plane that determines the relationship between a change in surface height and the resulting interferometric phase shift.

Figure 2 shows the surface as the camera sees it, with its view of the vectors $\hat{a}$, $\hat{b}$ and $\hat{\eta}$ superimposed on it. Since everything the camera sees is the projection of the three dimensional reality onto the plane perpendicular to the viewing direction, it is convenient to define three new vectors, which are just the projections of $\hat{a}$, $\hat{b}$ and $\hat{\eta}$ onto the viewing plane. If the viewing direction is $\hat{c}$, the projected vectors are:

$$\vec{u} = \hat{a} - (\hat{a} \cdot \hat{c})\,\hat{c} \tag{4}$$
$$\vec{v} = \hat{\eta} - (\hat{\eta} \cdot \hat{c})\,\hat{c} \tag{5}$$
$$\vec{w} = \hat{b} - (\hat{b} \cdot \hat{c})\,\hat{c} \tag{6}$$

From Figure 2, it is clear that the fringe intersections, which are what we normally refer to as the "fringes", are parallel to $\hat{u}$, but they are not perpendicular to either $\hat{v}$ or $\hat{w}$.

For now, we will assume that there is no additional information available -- the image of the surface with the fringes must be interpreted just as it is viewed. Thus, surface height deviations will be detected by deviations of the fringes from their parallel, uniformly spaced pattern. These fringe deviations can only be defined as the displacement of a fringe as measured perpendicular to the fringes, since there is no other directional information available.

Figure 3 shows the fringe pattern on an expanded scale, with a portion of one of the fringes being deviated due to a step change in surface height. Recall from Sensitivity I. that the physical spacing of the fringes as measured in the plane of the surface is defined as δ_p, where δ_f is the spacing between the fringe planes as measured along $\hat{s}$:

$$\delta_p = \frac{\delta_f}{|\hat{n} \times \hat{s}|} \tag{7}$$

Thus, the vector distance from one fringe to the next is simply $\delta_p \hat{b}$. In the viewing plane this vector fringe separation will appear as $\delta_p \vec{w}$. The apparent spacing of the fringes on the viewing plane is the distance x, which is measured perpendicular to the fringes as viewed. From the triangle on Figure 3 we can write:

$$x = \delta_p |\vec{w}| \sin \varphi \tag{8}$$

but

$$\cos \varphi = -\frac{\vec{w} \cdot \vec{u}}{|\vec{w}| |\vec{u}|} \tag{9}$$

thus

$$x = \delta_p \left[\frac{|\vec{w}|^2 |\vec{u}|^2 - (\vec{w} \cdot \vec{u})^2}{|\vec{u}|^2} \right]^{\frac{1}{2}} \tag{10}$$

Likewise, in Sensitivity I. we defined the shift in surface height as measured along $\hat{n}$ as ε and we defined the physical shift of a fringe intersection as the vector p $\hat{\eta}$. In this report we change the notation for the quantity p to ε_p (for symmetry); thus:

$$\varepsilon_p = \frac{\varepsilon}{|\hat{n} \times \hat{s}|} \tag{11}$$

The vector shift of the fringe intersection is $\varepsilon_p \hat{\eta}$, and in the viewing plane it will appear as a fringe shift $\varepsilon_p \vec{v}$. From Figure 3, the apparent shift of the fringe as measured perpendicular to the fringes is y. Repeating the same analysis as given by (8) to (10) we find:

$$y = \varepsilon_p \left[\frac{|\vec{v}|^2 |\vec{u}|^2 - (\vec{v} \cdot \vec{u})^2}{|\vec{u}|^2} \right]^{\frac{1}{2}} \tag{12}$$

Clearly, the magnitude of the phase shift corresponding to the fringe shift is:

$$|\Delta\phi| = 2\pi\left(\frac{y}{x}\right) \tag{13}$$

in radians. This becomes:

$$|\Delta\phi| = \frac{2\pi\varepsilon}{\delta_f}\left[\frac{|\vec{v}|^2|\vec{u}|^2-(\vec{v}\cdot\vec{u})^2}{|\vec{w}|^2|\vec{u}|^2-(\vec{w}\cdot\vec{u})^2}\right]^{\frac{1}{2}} \tag{14}$$

It is important for us to understand the **sign** of the phase shift as well as its magnitude. We choose the positive phase direction as the direction of $\hat{s}$. That is, the phase of each of the fringe surfaces increases by 2π from one surface to the next one as we go in the $\hat{s}$ direction. Now consider Figure 1 again, but this time imagine that the fringe surfaces are fixed in space and that the surface being inspected is rotated to various orientations. By the definition (2), we can see that vector $\hat{b}$ is just the vector component of $\hat{s}$ that lies in the plane of the surface. Thus, $\hat{b}$ is always oriented toward the positive phase direction. If $\hat{b}$ points toward positive phase, then so does its projection $\hat{w}$. So, the phase deviation for the case shown in Figure 3 is negative.

To generalize, the phase shift should be considered positive if y is in the same direction as x, and negative if it is in the opposite direction. If we write x and y as vectors, we have:

$$\hat{x} = \delta_p\left(\vec{w} - \frac{\vec{w}\cdot\vec{u}}{|\vec{u}|^2}\vec{u}\right) \tag{15}$$

$$\hat{y} = \varepsilon_p\left(\vec{v} - \frac{\vec{v}\cdot\vec{u}}{|\vec{u}|^2}\vec{u}\right) \tag{16}$$

and the sign of the phase shift is the sign of the quantity $(\hat{x}\cdot\hat{y})$. The complete expression for the phase shift then becomes:

$$\Delta\phi = \frac{2\pi\varepsilon}{\delta_f}\,\mathrm{SGN}\left[\vec{w}\cdot\vec{v} - \frac{(\vec{w}\cdot\vec{u})(\vec{u}\cdot\vec{v})}{|\vec{u}|^2}\right]\left[\frac{|\vec{v}|^2|\vec{u}|^2-(\vec{v}\cdot\vec{u})^2}{|\vec{w}|^2|\vec{u}|^2-(\vec{w}\cdot\vec{u})^2}\right]^{\frac{1}{2}} \tag{17}$$

After some algebra, the quantity in the last set of brackets in expressions (14) and (17) can be written:

$$Q = \frac{1 - (\hat{\mathbf{a}} \cdot \hat{\mathbf{c}})^2 - (\hat{\eta} \cdot \hat{\mathbf{c}})^2}{1 - (\hat{\mathbf{a}} \cdot \hat{\mathbf{c}})^2 - (\hat{\mathbf{b}} \cdot \hat{\mathbf{c}})^2} \tag{18}$$

where, for instance:

$$|\Delta\phi| = \frac{2\pi\varepsilon}{\delta_f}\sqrt{Q} \tag{19}$$

The expression for Q is considerably more lengthy if written in terms of $\hat{\mathbf{n}}$ and $\hat{\mathbf{s}}$.

Application

To check expression (19), first consider the case $\hat{\mathbf{c}} = \pm\hat{\eta}$. Then, since $\hat{\mathbf{a}} \cdot \hat{\eta} = 0$ by definition, $Q = 0$. This agrees with what we expect from the application of Equation (8) of Sensitivity I.

Next, consider the case when $\hat{\mathbf{s}} \cdot \hat{\mathbf{c}} = 0$. In this case, the view is coincident with the fringe planes. Here, we would expect that the phase shift would always be zero, since any deviation of the surface would cause a deviation of the fringe intersection that was parallel to the direction of the fringes as viewed. In other words, the fringe intersections must be viewed as straight lines when the view is contained in the plane of the fringes, no matter what the shape of the surface happens to be. To show that this is the case, we first write the view vector as a sum of the two perpendicular unit vectors that are also contained in the plane of the fringes:

$$\hat{\mathbf{c}} = \alpha\,\hat{\mathbf{a}} + \beta\,\hat{\eta} \tag{20}$$

where $\alpha^2 + \beta^2 = 1$. Plugging (20) into (18) we find:

$$Q = \frac{1 - \alpha^2 - \beta^2}{1 - \alpha^2 - \beta^2\,(\hat{\mathbf{b}} \cdot \hat{\eta})^2} = 0 \tag{21}$$

as expected.

When we calculated the motion of the fringe intersection in Equation (9) of Sensitivity I. , the apparent change in fringe intersection was zero only for the specific case of $\hat{\mathbf{c}} = \pm\hat{\eta}$. That is, if $\hat{\mathbf{c}}$ has some other orientation, even though confined to the plane of the fringes, the motion of the fringe intersection will be seen "in profile", and

will not in general be zero. The result (21) shows that we have made an important generalization of the work contained in that report.

Finally, consider the phase shift when $\hat{c} = -\hat{n}$, i.e, when the view is perpendicular to the surface under inspection. Since $\hat{a}\cdot\hat{n}$ and $\hat{b}\cdot\hat{n}$ are both zero by definition,

$$Q = 1 - (\hat{\eta}\cdot\hat{n})^2 \tag{22}$$

$$Q = 1 - \left[\frac{1 - (\hat{n}\cdot\hat{s})^2}{\sqrt{1 - (\hat{n}\cdot\hat{s})^2}}\right]^2 \tag{23}$$

$$Q = (\hat{n}\cdot\hat{s})^2 \tag{24}$$

and thus

$$|\Delta\phi| = \frac{2\pi\varepsilon}{\delta_f}\cos\theta \tag{25}$$

where θ was defined in Sensitivity I. Expression (25) is identical with Equation (16) of that report.

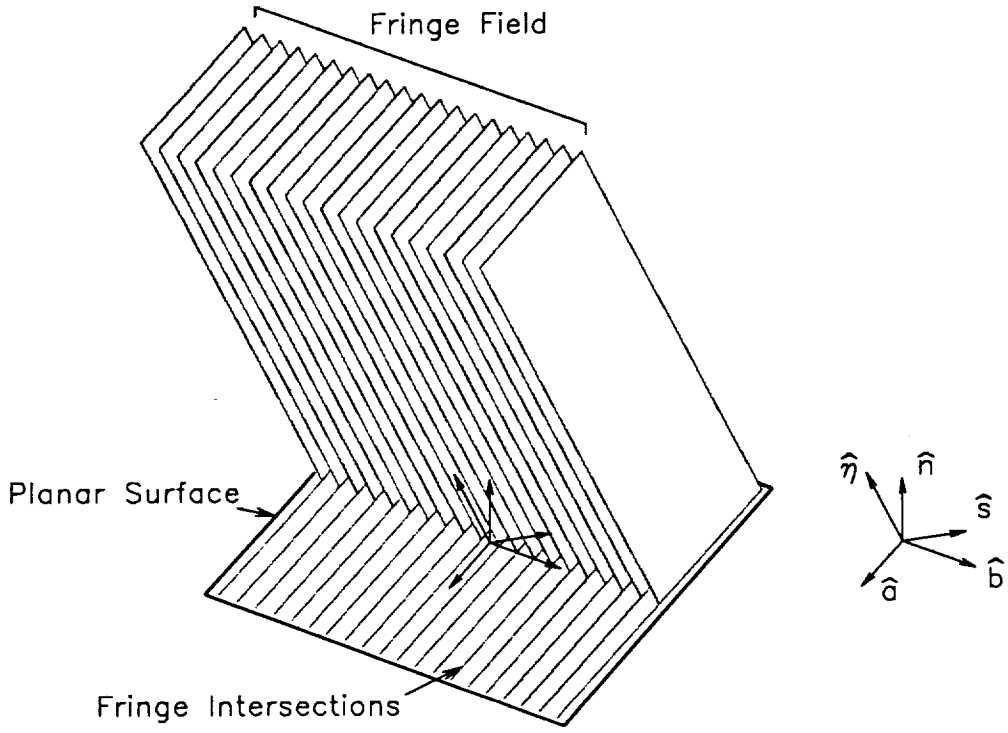

The geometry of projected fringe surface contouring.

FIGURE 1

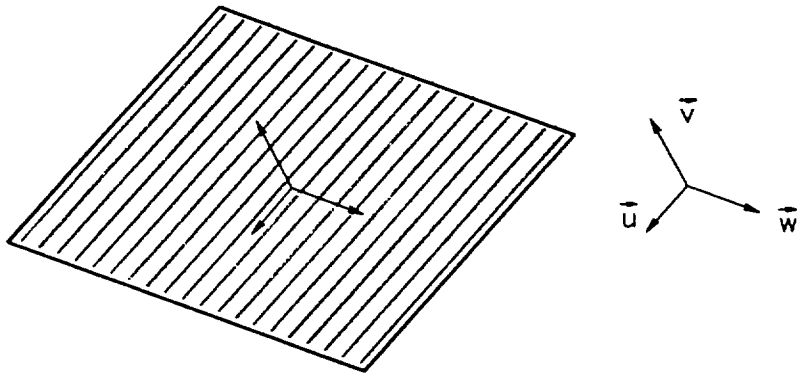

The camera's view of the surface with "fringes" and projected unit vectors.

FIGURE 2

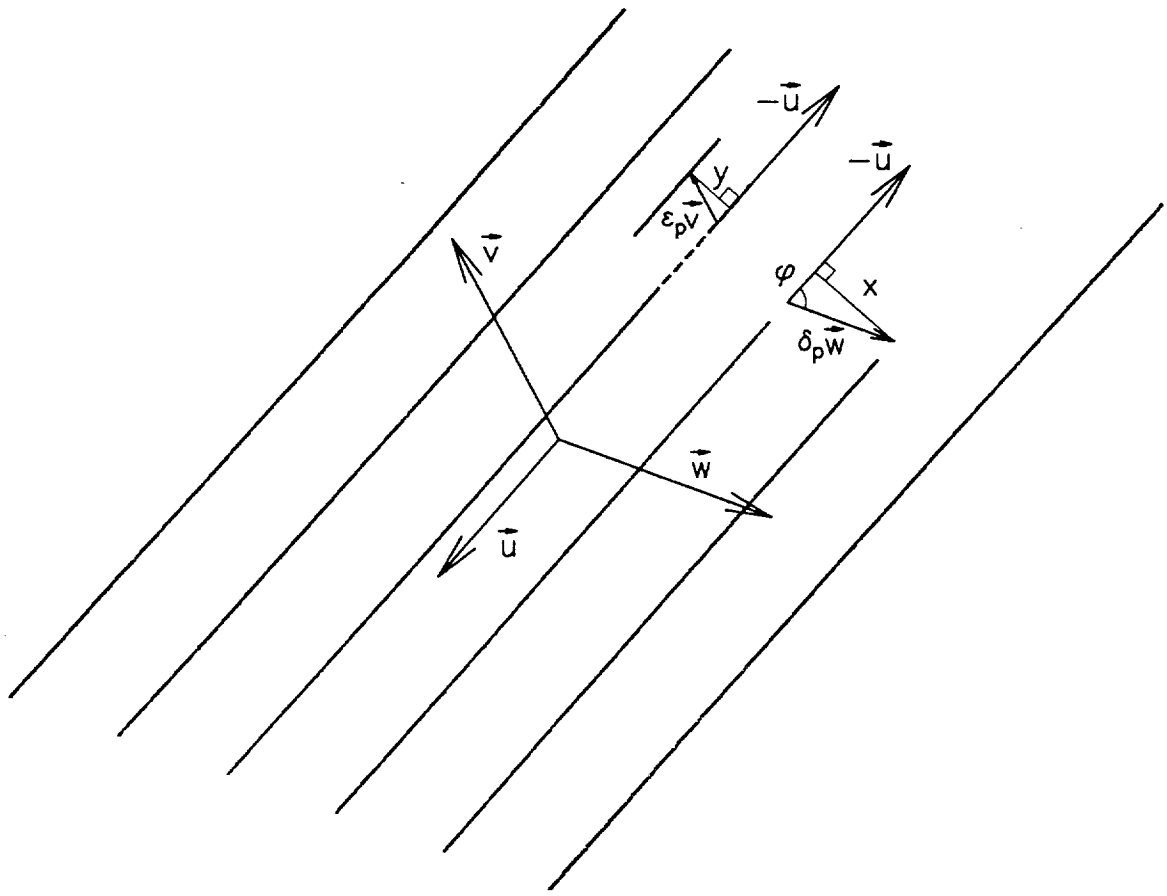

Fringe Deviation as Viewed

FIGURE 3